J|A|C|S
ARTICLES
Published on Web 04/27/2006

$C_{64}H_4$: Production, Isolation, and Structural Characterizations of a Stable Unconventional Fulleride

Chun-Ru Wang,*,† Zhi-Qiang Shi,† Li-Jun Wan,† Xin Lu,*,‡ Lothar Dunsch,*,§ Chun-Ying Shu,† Ya-Lin Tang,† and Hisanori Shinohara||

Contribution from the Beijing National Laboratory for Molecular Sciences (BNLMS), Institute of Chemistry, Chinese Academy of Sciences, Beijing 100080, China, State Key Laboratory for Physical Chemistry of Solid Surfaces and Department of Chemistry, Xiamen University, Xiamen 361005, China, Leibniz-Institut für Festkörper- and Werkstofforschung, Helmholtzstrasse 20, D-01171 Dresden, Germany, and Department of Chemistry and Institute for Advanced Research, Nagoya University, Nagoya 464-8602, Japan

Received October 4, 2005; E-mail: crwang@iccas.ac.cn; xinlu@xmu.edu.cn; l.dunsch@ ifw-dresden.de

Abstract: Unconventional fullerenes are those smaller than C_{60} or those intermediate between C_{60} and C_{70}, which are not stable in structure as none of the unconventional fullerene isomers satisfying the "isolated-pentagon-rule" (IPR). Below we report the synthesis of a stable unconventional fullerene derivative $C_{64}H_4$ by introducing methane in the fullerene productions with the normal Krätschmer−Huffman method. We also applied various spectroscopic measurements such as mass spectrometry, ^{13}C NMR, IR, UV−vis absorption spectrometry, etc. to characterize the structural and electronic properties of this molecule, revealing an unprecedented fullerene cage with a triplet of directly fused pentagons in the framework of $C_{64}H_4$. Four hydrogen atoms are added to the carbons at vertexes of fused pentagons to allow the bond angles at these sites close to the sp^3 tetrahedral angle, which essentially release the sp^2 bond strains on the abutting-pentagon sites of C_{64}. Ab initio calculations were performed to explore the electronic property and simulate the ^{13}C NMR and IR spectra of this fulleride, which reproduced well the experimental results and confirmed the structural assignment of the $C_{64}H_4$.

1. Introduction

Fullerenes are closed-cage carbon polyhedrons that are composed of 12 pentagons and an uncertain number of hexagons. With this definition the possible fullerenes should begin from C_{20};[1] however, due to the limitation of the "isolated-pentagon-rule" (IPR)[2] which rules out those fullerene structures containing fused pentagons, the first stable fullerene is in fact C_{60} and the second one is C_{70}. Except for C_{36},[3] whose synthesis and isolation are still in debate,[4,5] most of the other small fullerenes (i.e., C_{20}−C_{58}, C_{62}−C_{68}) are neither stable in structure nor isolable macroscopically,[5] so they were defined as unconventional fullerenes. In fullerene studying, the unconventional fullerenes show also great significances as normal fullerenes do. First, unconventional fullerenes provide valuable clues about how the fullerenes grow up because they are precursors of conventional fullerenes (e.g., C_{60}, C_{70}, etc.) in growing according to the "fullerene road" mechanism.[6] Second, several recent papers[7,8] reported the synthesis, isolation, and characterizations of some stable metallofullerenes[7] or fullerene derivatives[8] based on C_{50}, C_{66}, and C_{68}, implying that these unconventional fullerenes can be essentially stabilized by either endohedral or exohedral derivatization. Chemists are highly interested in why and how these otherwise extremely unstable fullerene species were stabilized. Finally, some unconventional fullerene materials, e.g., the solid of C_{36}[3] and Ce@C_{44}, etc.[9] were revealed to own novel electronic properties and superconductivity, so they may be found in direct applications in future.

It is well-known that fullerenes composed of all sp^2 hybridized carbons are somewhat similar to the graphite. Since sp^2 carbon adopts preferentially a *planar* trigonal symmetry in nature, obviously, even the most stable IPR-satisfying fullerenes such as C_{60} and C_{70} would deviate from the planar carbon sp^2

† Institute of Chemistry, Chinese Academy of Sciences.
‡ Xiamen University.
§ Leibniz-Institut für Festkörper- and Werkstofforschung.
|| Nagoya University.

(1) Fowler, P. W.; Manolopoulos, D. E. *An Atlas of Fullerenes*; Clarendon: Oxford, 1995.
(2) Kroto, H. W. *Nature* **1987**, *329*, 529−531.
(3) Piskoti, C.; Yarger, J.; Zettl, A. *Nature* **1998**, *393*, 771−774.
(4) (a) Koshio, A.; Inakuma, M.; Sugai, T.; Shinohara, H. *J. Am. Chem. Soc.* **2000**, *122*, 398−399. (b) Koshio, A.; Inakuma, M.; Wang, Z. W.; Sugai, T.; Shinohara, H. *J. Phys. Chem. B* **2000**, *104*, 7908−7913.
(5) Lu, X.; Chen, Z. *Chem. Rev.* **2005**, *105*, 3643−3696 and references therein.
(6) (a) Heath, J. R. *Fullerenes*; ACS Symposium Series 481; American Chemical Society: Washington, DC, 1992. (b) Heath, J. R. *Nature* **1998**, *393*, 730−731. (c) Shvartsburg, A. A.; Hudgins, R. R.; Dugourd, P.; Gutierrez, R.; Frauenheim, T.; Jarrold, M. F. *Phys. Rev. Lett.* **2000**, *84*, 2421−2424. (d) Lu, W. Y.; Huang, R. B.; Ding, J. Q.; Yang, S. H. *J. Chem. Phys.* **1996**, *104*, 6577. (e) Bates, K. R.; Scuseria, G. E.; *J. Phys. Chem. A* **1997**, *101*, 3038−3042.
(7) (a) Wang, C.-R.; Kai, T.; Tomiyama, T.; Yoshida, T.; Kobayashi, Y.; Nishibori, E.; Takata, M.; Sakata, M.; Shinohara, H. *Nature* **2000**, *408*, 426−427. (b) Stevenson, S.; Fowler, P. W.; Heine, T.; Duchamp, J. C.; Rice, G.; Glass, T.; Harich, K.; Hajdu, E.; Bible, R.; Dorn, H. C. *Nature* **2000**, *408*, 428−429. (c). Shi Z. Q.; Wu, X.; Wang C. R.; Lu X.; Shinohara, H. *Angew. Chem., Int. Ed.* **2006**, *45*, 2107−2111.
(8) Xie, S. Y.; Gao, F.; Lu, X.; Huang, R. B.; Wang, C. R.; Zhang, X.; Liu, M. L.; Deng, S. L.; Zheng, L. S. *Science* **2004**, *304*, 699−670.
(9) Klingeler, R.; Breuer, C.; Wirth, I.; Blanchard, A.; Bechthold, P. S.; Neeb, M.; Eberhardt, W. *Surf. Sci.* **2004**, *553*, 95−104

Scheme 1

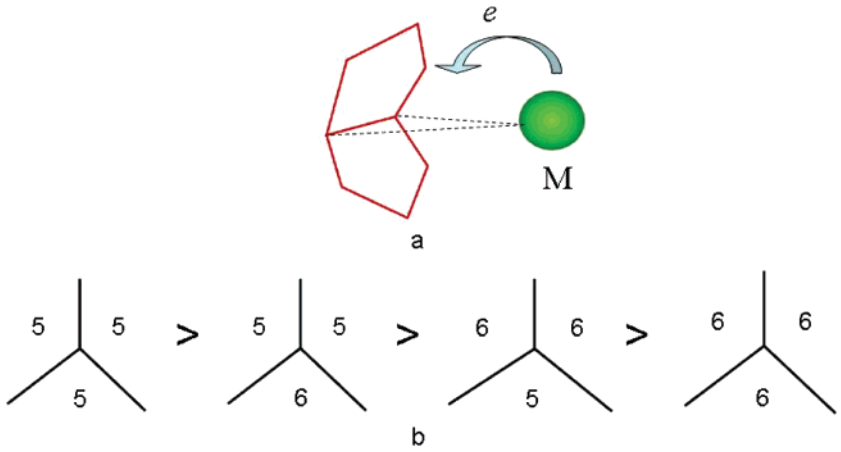

symmetry and induce slight bond strains, not to say unconventional fullerenes in which the carbons at vertexes of abutting pentagons would deviate far from the sp^2 hybridizations. Hence huge bond strains are expected at the IPR-violating fullerenes. However, inasmuch the bond strains are localized in fused pentagon sites, then if special actions were performed aiming at the fused pentagons, e.g., by interacting with encaged metal or by chemically modifying the carbons at vertexes of fused pentagons, it is possible to essentially release the bond strains there and get stable structures as metallofullerenes or fullerene derivatives.

Recently, several endohedral unconventional metallofullerenes,[7] e.g., $Sc_2@C_{66}$, $Sc_3N@C_{68}$, and $Sc_2C_2@C_{68}$, etc., were synthesized and characterized, which may be taken as prototype molecules to find out how the bond strains of fused pentagons are able to be largely decreased in the metallofullerene case. As shown in Scheme 1a, a typical M-(pentagon × 2) structure can be derived from these endohedral unconventional fullerenes, implying that the metal atom must bond to the fused-pentagon pair tightly in allusion to decrease the localized bond strains of fused pentagons by electron transfer. As a comparison, it should be mentioned that the metal atoms in most other metallofullerenes usually show free dynamic movements inside the fullerene cages.[10] Moreover, it was recently disclosed that metallofullerenes $M_2@C_{72}$[11] (M = Sc and La) also contain such a M−(pentagon × 2) structure, indicating that this type of structure can release the bond strains of abutting pentagons independent of the metal and fullerene size.

Another way to mitigate the bond strains of fused pentagons is to change the hybridizations of the carbons at vertexes of abutting pentagons from sp^2 to sp^3 by chemically modifying the fullerenes. Due to the large difference between the sp^3 tetrahedral and planar sp^2 trigonal angles, the transition from sp^2 to sp^3 will obviously benefit some typical structure of unconventional fullerenes to release the bond strains and form stable unconventional fullerene derivatives. In the past decade, extensive theoretical studies have been performed to explore some important unconventional fullerene derivatives. For example, Choho et al.[12] studied the stability of C_{28} and C_{28} derivatives, revealing that C_{28} derivatives (e.g., $C_{28}H_4$) are much more stable than C_{28}. Lin et al.[13a] and Xiao et al.[13b] calculated several unconventional fullerenes C_{28}−C_{40} and found a stability order for hydrogen addition of fullerenes at different carbon sites as shown in Scheme 1b. Xu et al.[14] calculated several isomers of C_{50} and $C_{50}H_{2n}$, suggesting a low energetic structure of $C_{50}H_{10}$ (D_{5h}) in which 10 hydrogen atoms were added to the 5/5 fused pentagon sites of C_{50}. Recently, the first stable unconventional fullerene derivative of C_{50}, $C_{50}Cl_{10}$, was successfully synthesized and isolated by Xie et al.[8] The high stability of this compound clearly evidences that the large steric strains pertaining to the fused pentagons are effectively released by covalent attachment of Cl atoms to the 10 carbons at the vertexes of fused-pentagon sites of C_{50} (D_{5h}).

In this paper, we report the synthesis and structural characterizations of a new unconventional fullerene derivative, $C_{64}H_4$. The synthesis of this molecule not only provides another prototype of stable unconventional fullerene derivatives other than $C_{50}Cl_{10}$, enabling us to witness how the sp^3 hybridized carbons work to release the bond strains of triplet abutting pentagons, but also is of great significance in studying the fullerene growth mechanism from C_{60} to C_{70}.

2. Results and Discussions

2.1. Synthesis and Purification. $C_{64}H_4$ was synthesized by arc-burning pure graphite rods (φ8 × 200 mm) in a direct current mode (12 V, 170 A) under 500 Torr helium/methane mixture atmosphere (95:5 in volume ratio);[10a,15] here the methane was added to provide as a hydrogen source. The $C_{64}H_4$-containing soot was collected and Soxhlet extracted by toluene for 24 h. The purification and isolation of $C_{64}H_4$ were achieved by multistep high-performance liquid chromatography (HPLC) with two complimentary columns, i.e., the Buckyprep column (20 mm × 250 mm, Cosmosil) and the Buckyclutscher column (21.1 mm × 500 mm, Regis Chemical). The retention time of

(10) (a) Shinohara, H. *Rep. Prog. Phys.* **2000**, *63*, 843−892. (b) Krause, M.; Hulman, M.; Kuzmany, H.; Dubay, O.; Kresse, G.; Seifert, G.; Wang, C.-R.; Shinohara, H. *Phys. Rev. Lett.* **2004**, *93*, 137403. (c) Akasaka, T.; Nagase, S.; Kobayashi, K.; Wälchli, M.; Yamamoto, K.; Funasaka, H.; Kako, M.; Hoshio, T.; Erata, T. *Angew. Chem., Int. Ed.* **1997**, *36*, 1643−1645.
(11) Kato, H.; Taninaka, A.; Sugai, T.; Shinohara, H. *J. Am Chem. Soc.* **2003**, *125*, 7782−7783.
(12) Choho, K.; Woude, G. V. D.; Lier, G. V.; Geelings, P. *THEOCHEM* **1997**, *417*, 265−276.
(13) (a) Lin, M. H.; Chiu Y. N.; Xiao J. M. *THEOCHEM* **1999**, *489*, 109−117. (b) Xiao, J. M.; Lin, M. H.; Chiu, Y. N.; Fu, M. Z.; Lai, S. T.; Li, N. N. *THEOCHEM* **1998**, *428*, 149−154.
(14) Xu, W. G.; Wang, Y.; Li, Q. S. *THEOCHEM* **2000**, *531*, 119−125.
(15) (a) Krätschmer, W.; Lamb, L. D.; Fostiropoulos, K.; Huffman, D. R.; *Nature* **1990**, *347*, 354−357. (b) Kato, H.; Taninaka, A.; Sugai, T.; Shinohara, H. *J. Am. Chem. Soc.* **2003**, *125*, 7782−7783.

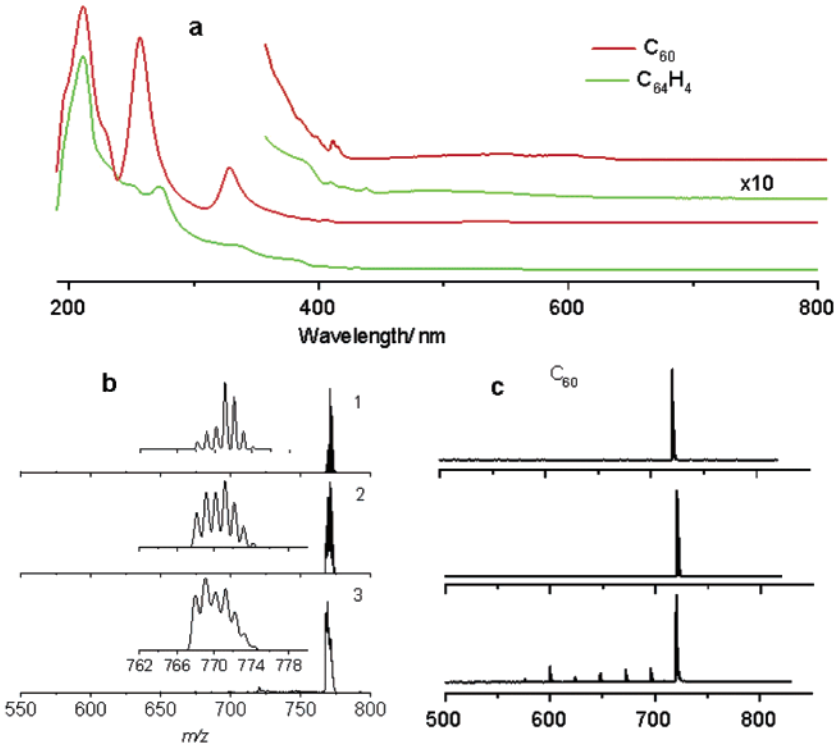

Figure 1. (a) UV/visible absorption spectra of C_{60} and $C_{64}H_4$. (b) Mass spectrometry studies of $C_{64}H_4$. Fragments corresponding to 1−4 hydrogen atom loss from $C_{64}H_4$ are always observed; along with enhancing laser power [**1**: 75 (laser intensity in arbitrary unit); **2**:100; **3**: 105], the molecule tends to lose more hydrogen atoms. While the laser power is high enough (**3**), fragments corresponding to the trace of C_{60} are observed. (c) Mass spectrometry study of C_{60} decomposition behavior in the same laser power sequences as shown in part b.

$C_{64}H_4$ in the Buckyprep column is located between that of C_{60} and C_{70} (Figure S1), so the Buckyprep column was used in step 1 to collect the $C_{64}H_4$-containing fraction and remove normal fullerenes such as C_{60}, C_{70}, C_{76}, C_{84}, etc. It was estimated that the relative yield of $C_{64}H_4$ is ca. 0.2% of that of C_{60}, so we repeated step 1 many times to enrich the $C_{64}H_4$ sample. In step 2 the enriched $C_{64}H_4$ sample was reinjected into the Buckyprep column, and recycling was performed to remove impurities from C_{60} derivatives such as $C_{60}O$, $C_{60}O_2$, etc. Step 3 is again a recycling process in the Buckyclutscher column, which further purifies the sample up to 99% in purity.[16] Finally, ca. 3 mg of $C_{64}H_4$ sample was collected for spectroscopic characterizations.

2.2. Structural Characterizations. $C_{64}H_4$ dissolves well in toluene and carbon disulfide. It shows a purplish-red color in CS_2 solution that is slightly different from the purple color of C_{60}. Figure 1a gives a comparison of the UV−visible absorption spectra of $C_{64}H_4$ and C_{60} in hexane. The characteristic feature of $C_{64}H_4$ is observed essentially similar to that of C_{60}. C_{60} shows known characteristic absorption peaks at 210, 256, 328, and 405 nm, whereas the absorptions of $C_{64}H_4$ are located at 210, 247, 273, 340, 383, and 431 nm. Strikingly, the onset of $C_{64}H_4$ is nearly the same as that of C_{60}, suggesting that this molecule is a wide band gap fullerene such as C_{60}.[17]

Matrix assist laser desorption ionization mass spectroscopic (MALDI-MS) studies of the $C_{64}H_4$ sample indicate that the molecule can lose 1−4 hydrogen atoms under laser desorption/ionization (Figure 1b), suggesting the hydrogen atoms must be exohedrally attached to the carbon cage. We try to further fragment the $C_{64}H_4$ molecule by continuously increasing the laser intensity, and it was observed that the $C_{64}H_4$ molecule tends to lose more hydrogen atoms (Figure 1b1 and 1b2) but no other chemical groups are stripped off from the molecule, so the molecular framework should be C_{64} but not C_{60}. It is not until the laser power is high enough to break down the C_{60} cage as revealed by a parallel experiment for C_{60} (Figure 1c) that only a trace of C_{60} fragments appears in the mass spectrum of $C_{64}H_4$ (Figure 1b3), suggesting the high stability of the $C_{64}H_4$ framework which is comparable to that of C_{60}.

The geometric structure and the molecular symmetry of $C_{64}H_4$ are studied by means of NMR spectroscopy on a Bruker AV600 spectrometer. Figure 2a shows a 125 MHz ^{13}C NMR spectrum of $C_{64}H_4$ in CS_2 solution and locked by acetone-d_6 at room temperature. A total of 14 distinct signals appear in the spectrum; 12 peaks are located at the sp^2-hybridizing range (125−160 ppm), and the other 2 peaks (57.29 and 55.76 ppm) are located in the sp^3-hybridizing range.

Because C_{60} is the smallest IPR-satisfied fullerene and C_{70} is the second, C_{64} must violate the IPR.[2] Out of the 3464 non-IPR isomers of C_{64} calculated by the spiral algorithm,[1] there is only one C_{3v}-C_{64} isomer that fits the observed ^{13}C NMR pattern [$sp^2(8 \times 6; 4 \times 3)$; $sp^3(1 \times 3; 1 \times 1)$, where ($a \times b$) indicates "$a$" group of "$b$" symmetrical equivalent carbon atoms]. We thus build the $C_{64}H_4$ molecular structure as shown in Figure 3 based on the C_{3v}-C_{64} and NMR data. The proposed structure includes a triple fused-pentagon group, and four hydrogen atoms were bonded in the fused pentagonal site to lower the bending energies of fused pentagons. Obviously, the former 12-peak

(16) The purity of $C_{64}H_4$ was confirmed by both HPLC and TOF mass spectrometry. For example, Figure S2 shows a recycling HPLC profile to purify the sample with a buckyprep column. A single peak was observed from the 3rd cycle to more than 20th cycles, implying a high purity of the sample after purification process.

(17) Wang, C. R.; Inakuma, M.; Shinohara, H. *Chem. Phys. Lett.* **1999**, *300*, 379−384.

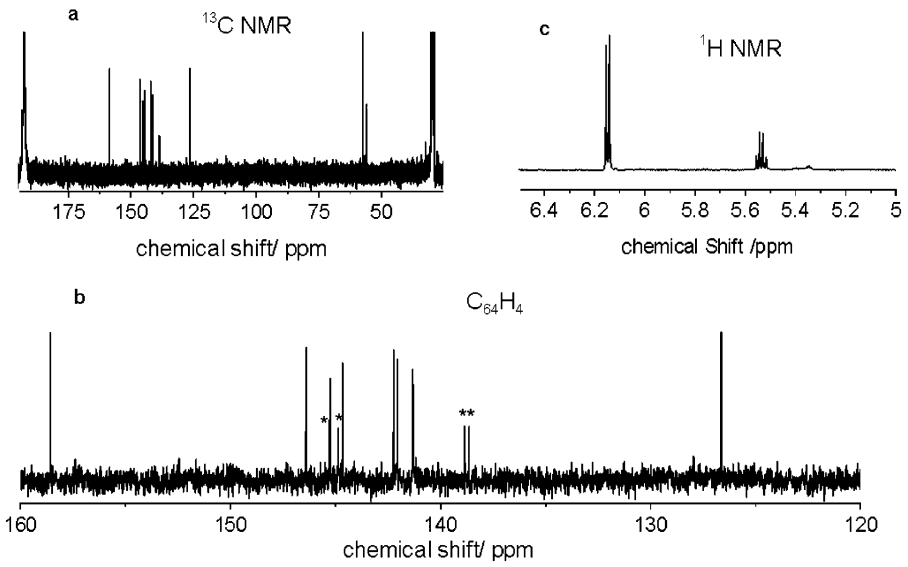

Figure 2. (a) ^{13}C NMR spectrum of $C_{64}H_4$ in CS_2 solution, acetone-d_6 lock at room temperature. (b) The sp^2 hybridizing carbon range of the ^{13}C NMR spectrum of $C_{64}H_4$. (c) ^{1}H NMR spectrum of $C_{64}H_4$, $^3J_{H-H} = 7.8$ Hz.

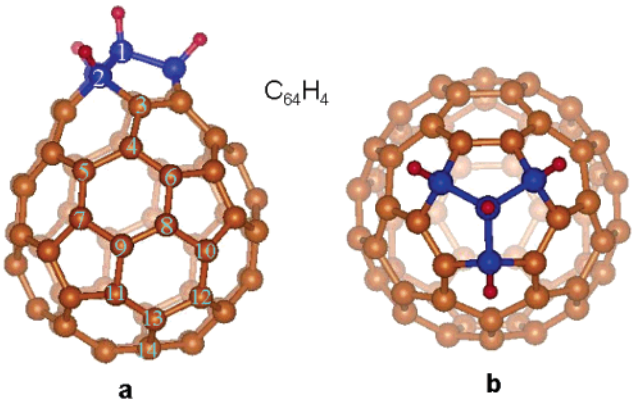

Figure 3. Two views of the molecular structure of $C_{64}H_4$. The red balls represent hydrogen atoms, the pink balls represent sp^2 carbon atoms, and blue balls represent sp^3 carbon atoms. The structural model is constructed based on NMR studies and optimized by ab initio calculations at the B3LYP/6-31G* theoretical level.

group [$sp^2(8 \times 6; 4 \times 3)$], as shown in Figure 2b, of NMR lines are attributed to the 60 sp^2 hybridized carbon atoms of $C_{64}H_4$ outside of the fused pentagonal sites, in which 8 lines have nearly equal intensity and the other 4 lines are half of the intensity. The latter 2-peak group [$sp^3(1 \times 3; 1 \times 1)$] is attributed to the four sp^3 hybridized carbon atoms of $C_{64}H_4$ in the fused-pentagon site, in which the two lines have a relative intensity of 3:1.

Figure 2c shows a 600 MHz ^{1}H NMR spectrum of the species on a Bruker AV600 spectrometer, in which two signals are observed in an intensity ratio of ca. 3:1. A high resolution ^{1}H NMR spectroscopic study shows that the higher signal is a doublet (6.142 and 6.155 ppm) and the lower signal is a quartet (5.517, 5.530, 5.543, 5.556 ppm) split due to the ^{1}H−^{1}H coupling. Considering the C_{3v} symmetry of $C_{64}H_4$ and the relative intensity of NMR signals, we can easily assign the doublet signals as due to the three equivalent H atoms out of the main C_3 axis of $C_{64}H_4$, whereas the quartet signals can be assigned as the single H atom along the main C_3 axis. Two-dimensional Heteronuclear Multiple Quantum Coherence (2D-HMQC) NMR measurements were performed and confirmed

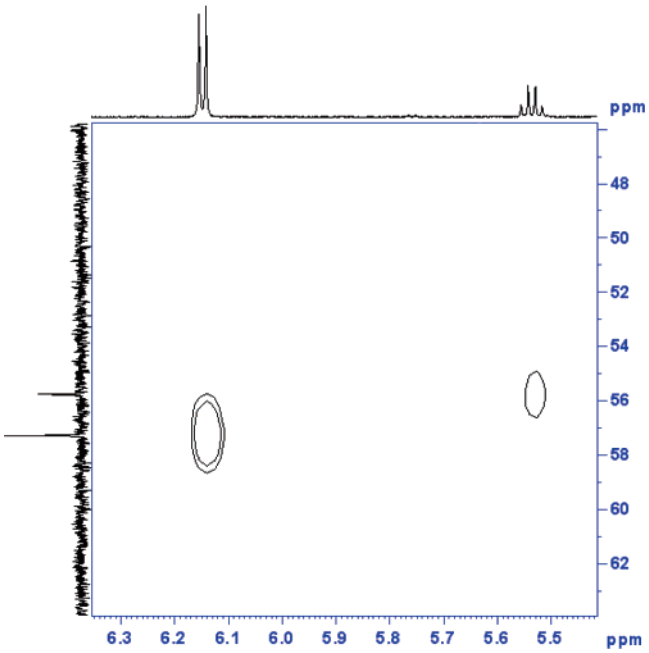

Figure 4. Selected range of 2D-HMQC ^{1}H−^{13}C NMR spectrum.

the connectivity between the four sp^3 hybridized carbon atoms and the four hydrogen atoms (Figure 4).

2.3. Theoretical Simulations. To assign the NMR spectra, we performed ab initio calculations using the Gaussian 03W program.[18] ^{13}C nuclear magnetic shielding tensors of the C_{3v}-$C_{64}H_4$ molecule were calculated at the GIAO-B3LYP[19]/6-31G* level of theory with the geometry optimized at the same level. Based on the predicted ^{13}C nuclear magnetic shielding tensors, the ^{13}C chemical shifts were computed relative to C_{60} and converted to the tetramethylsilane scale using the experimental value for C_{60} ($\delta = 142.5$ ppm). As shown in Figure 5 and Tables 1 and 2, the computed chemical shifts of $C_{64}H_4$ are well

(18) Frisch, M. J.; et al. *Gaussian 03*; Gaussian, Inc.: Pittsburgh, PA, 2003.
(19) For the hybrid density functional B3LYP method, see: Becke, A. D. *J. Chem. Phys.* **1993**, *98*, 5648. Lee, C.; Yang, W.; Parr, R. G. *Phys. Rev. B* **1988**, *37*, 785−796.

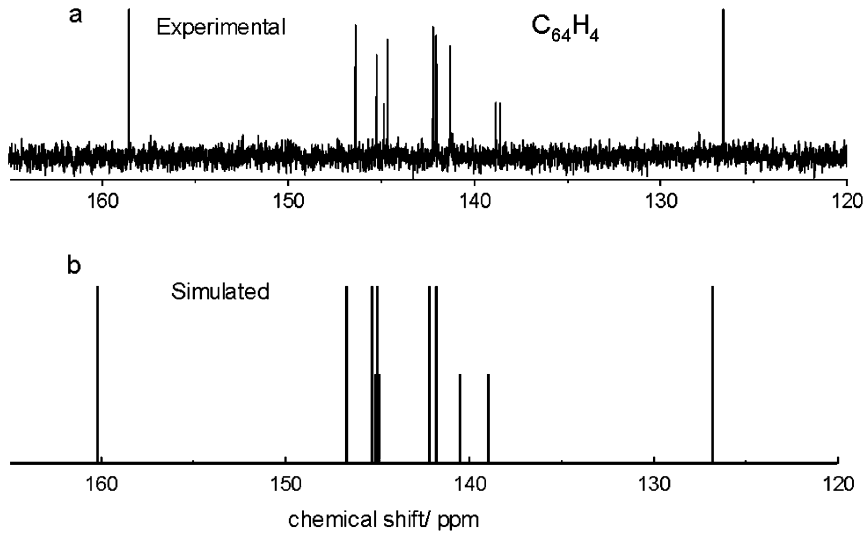

Figure 5. Experimental and theoretically calculated ^{13}C NMR spectrum of $C_{64}H_4$ by ab initio calculations at the B3LYP/6-31G* level.

Table 1. Experiment and Theoretical ^{13}C NMR Chemical Shifts (δ, ppm)[a] of $C_{64}H_4$

no.[b]	δ/ppm (exptl)	intensity	δ/ppm (calcd)
1	55.8	1	61.2
2	57.2	3	62.4
3	159.0	6	160.2
4	126.6	6	126.8
5	138.8	3	140.5
6	141.3	6	141.8
7	138.6	3	139.0
8	142.0	6	141.8
9	142.2	6	142.2
10	145.3	3	145.1
11	145.4	6	145.3
12	144.9	3	144.9
13	144.7	6	145.0
14	146.4	6	146.7

[a] The ^{13}C chemical shifts were computed relative to C_{60} and converted to the tetramethylsilane scale using the experimental value for C_{60} (δ = 142.5 ppm). [b] See Figure 3a for definition of the atomic labels.

Table 2. Experimental and Calculated ^1H NMR Chemical Shifts (δ, ppm)[a] of $C_{64}H_4$

no.	δ/ppm (exptl)	intensity	δ/ppm (calcd)
1	5.5	1	5.0
2	6.1	3	5.9

[a] The ^1H chemical shifts were computed relative to benzene and converted to the tetramethylsilane scale using the experimental value for benzene (δ = 7.3 ppm).

consistent with the experimental results, confirming the proposed structure of $C_{64}H_4$. Based on the computational results, a quantitative assignment of the observed ^{13}C NMR lines are given in Table 1. In agreement with the UV−vis observation, the computed HOMO−LUMO gap of $C_{64}H_4$ (2.67 eV) is close to that of C_{60} (2.77 eV), showing that $C_{64}H_4$ is also a wide band gap fullerene.

The structural and electronic properties of $C_{64}H_4$ have been further characterized by infrared spectroscopy. In principle, the 144 vibrational modes of the C_{3v}-$C_{64}H_4$ molecule can be divided into three categories pertaining to 37 A_1 + 66 E + 29 A_2 symmetries. Among them the IR active vibrations are of A_1 and E symmetries. The experimental IR spectrum of $C_{64}H_4$ shows two major ranges, i.e., the C−H stretching modes at ca. 2900 cm^{-1} and a wide range of features located at <1800 cm^{-1} which include the C−C stretching, C−C−C bending, and C−C−H bending modes (Figure 6). The simulated IR spectrum based on theoretical vibrational frequencies predicted at the B3LYP/6-31G* theoretical level (Supporting Information) is also depicted in Figure 6. As shown in Figure 6, the calculated IR spectrum of the C_{3v}-symmetric $C_{64}H_4$ agrees well with the experimental one, providing further evidence of the non-IPR molecular structure of $C_{64}H_4$.

2.4. Discussions. As mentioned in section 2.1, 5% methane was introduced to produce the $C_{64}H_4$. Thus a large quantity of hydrogen atoms would exist in the arc-discharging chamber. However, we did not observe any other C_{64}-based fullerides except $C_{64}H_4$, and for $C_{64}H_4$ only the 5/5/5 and 5/5/6 sites were chemically modified as characterized above. This result is consistent with the theoretical expectation[13] that the stability order for hydrogen addition to carbon atoms at different sites of fullerene cages is 5/5/5 > 5/5/6 > 6/6/5 > 6/6/6 (Scheme 1b). Moreover, measured from the optimized structure of $C_{64}H_4$, the C−C−C bond angles at the 5/5/5 site are 106.0° and those at 5/5/6 sites are 105.3°, respectively. These angles are much closer to the sp^3 tetrahedral angles than to the planar trigonal sp^2 angles, so the large bond strains of sp^2 carbons at these sites are mitigated efficiently upon chemical modifications. This would be the reason $C_{64}H_4$ shows very high stability comparable to that of C_{60} and C_{70}.

The successful isolation of $C_{64}H_4$, together with previous isolated $C_{50}Cl_{10}$,[8] $Sc_2@C_{66}$,[7a] $Sc_3N@C_{68}$,[7b] and $Sc_2C_2@C_{68}$,[7c] etc. reveals the possibility of a stable structure based on unconventional fullerenes once the bond strains at fused pentagons were mitigated. Based on these results, one may extend the IPR to a general rule defined as the "minimization-of-bond-strain rule" (MBSR),[20] which sets a criterion for stable closed carbon cages that the bond strains should be minimized at every site of the carbon cages, no matter if the hybridization of carbon atoms in the framework of carbon cages is sp^2 or sp^3. IPR is in fact an ancillary condition of this rule that can be

(20) One of the referees contributes a lot on the idea of "minimization-of-bond-strain rule" who made in-depth discussions on the stability of different fullerene materials in his referee reports.

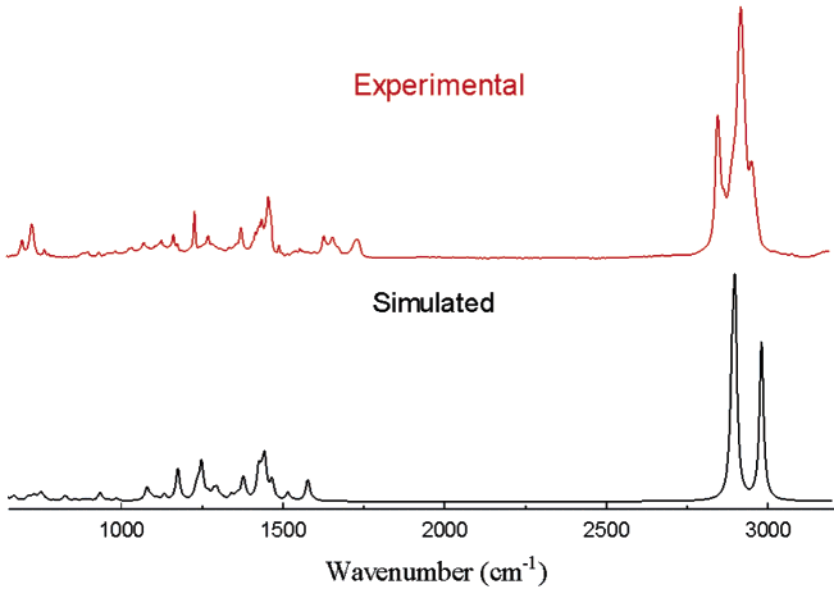

Figure 6. Experimental and simulated IR spectra of $C_{64}H_4$.

applied exclusively to intact fullerenes, but the MBSR may be used widely for fullerenes, endohedral fullerenes, exohedral fullerene derivatives, heterofullerenes,[21] and even fullerene derivatives containing four-membered rings[22] or seven-membered rings.[23] Take the $C_{64}H_4$ to explain the MBSR: the original C_{64} fullerene contains three abutting pentagons that bring huge bond strains to the fused pentagon sites, so C_{64} is unstable in structure. But once the four carbon atoms at vertexes of the fused pentagon sites were chemically modified by hydrogen additions, the sp^2 to sp^3 hybridization change of the vertex carbon atoms would release remarkably the bond strains, affording the high stability of the $C_{64}H_4$ structure.

The isolation of $C_{64}H_4$ is also very significant in exploring the fullerene formation mechanism. The widely accepted "fullerene road" mechanism[6] supposes that fullerenes grow in a carbon plasma by the addition of C_2 units successively. Note that the main framework of $C_{64}H_4$ is similar to that of C_{60}, it is most likely that this C_{64} bridges between C_{60} and C_{70} as one of the precursors of C_{70}. However, considering the high stability and low yield of $C_{64}H_4$ compared to that of C_{70}, the C_{64} structure would not be the only C_{64} intermediate leading to C_{70}, since otherwise the yield of $C_{64}H_4$ should be much higher to being at least similar to that of C_{70}. Given the fact that abundant unconventional fullerenes were observed in the raw soot,[24] it is most likely that a whole family of C_{64} isomers were made in the fullerene growing process, but all the others cannot be modified as stable fullerides except for the current $C_{64}H_4$. We look forward to further investigations to see if other unconventional fullerides such as $C_{66}H_x$ and $C_{68}H_x$ can be produced and isolated by similar experimental techniques.

Acknowledgment. C.R.W. thanks NSFC (Nos. 50225206, 90206045, 20121301), the Major State Basic Research Program of China "Fundamental Investigation on Micro-Nano Sensors and Systems based on BNI Fusion" (Grant 2006CB300402), and the National Center for Nanoscience and Technology of China. X.L. thanks NSFC (Nos. 20021002, 20425312, 20203013). The authors are indebted to referees for constructive suggestions.

Supporting Information Available: The HPLC separation of $C_{64}H_4$, full range 2D-HMQC NMR spectrum, the numbering of carbon atoms in C_{64}, and details of the calculated vibrational frenquencies, IR intensities of $C_{64}H_4$. This material is available free of charge via the Internet at http://pubs.acs.org.

JA0567844

(21) (a) Hummelen, J. C.; Knight, B.; Pavlovich, J.; González, R.; Wudl, F. *Science* **1995**, *269*, 1554−1556. (b) Nuber, B.; Hirsch, A. *Chem. Commun.* **1996**, *14*, 1421. (c) Keshavarz, K. M.; González, R.; Hicks, R. G.; Srdanov, G.; Srdanov, V. I.; Collins, T. G.; Hummelen, J. C.; Bellavia-Lund, C.; Pavlovich, J.; Wudl, F.; Holczer, K. *Nature* **1996**, *383*, 147−150.

(22) (a) Qian, W.; Bartberger, M. D.; Pastor, S. J.; Houk, K. N.; Wilkins, C. L.; Rubin, Y. *J. Am. Chem. Soc.* **2000**, *122*, 8333−8334. (b) Qian, W.; Chuang, S. C.; Amador, R. B.; Jarrosson, T.; Sander, M.; Pieniazek, S.; Khan, S. I.; Rubin, Y. *J. Am. Chem. Soc.* **2003**, *125*, 2066−2067.

(23) Troshin, P. A.; Avent, A. G.; Darwish, A. D.; Martsinovich, N.; Abdul-Sada, A. K.; Street, J. M.; Taylor, R. *Science* **2005**, *309*, 278−281.

(24) In raw soot of arc-discharging graphite a full range of C_{2n} ($2n > 48$) were observed by mass spectrometry. A typical mass spectrum of the raw soot was shown in Figure S5 in the Supporting Information.